The plasma observations from the flyby are rich in detail, showing that the outer regions of the Jovian magnetosphere are remarkably similar to those of Earth. We anticipate that, as the plasma observations are analyzed in greater detail and as joint studies with combined data sets from the various investigations are completed, new discoveries will be made and our understanding of Jupiter's magnetosphere will improve significantly.

REFERENCES AND NOTES

1. J. H. Wolfe, H. R. Collard, J. D. Mihalov, D. S. Intriligator, *Science* **183**, 303 (1974).
2. H. S. Bridge *et al.*, *ibid.* **204**, 987 (1979); H. S. Bridge *et al.*, *ibid.* **206**, 972 (1979).
3. E. J. Smith, K.-P. Wenzel, D. E. Page, *ibid.* **257**, 1503 (1992).
4. Both instruments utilize spherical section electrostatic analyzers that direct analyzed particles into arrays of channel electron multipliers for detection. Electrons are measured from 1.59 to 862 eV and ions from 256 eV per charge to 35 keV per charge. The electron spectrometer is oriented to cover a range of polar angle of ±73° with respect to the equator of the spinning spacecraft, a range suitable for both magnetospheric and solar wind electrons. The ion spectrometer is designed to detect the narrow, antisunward beam of solar wind ions over limited ranges of azimuth and polar angle; this is generally less suitable for magnetospheric ions, which have broad distributions, often have unfavorable flow directions, and usually have low flux intensities. Sets of counts are obtained every 5.7 min for electrons and 4 min for ions as a function of azimuth (spin angle), polar angle (channel electron multiplier number), and energy (analyzer voltage level). Pertinent plasma parameters such as number density and temperature are derived from these sets.
5. S. J. Bame *et al.*, in *The International Solar Polar Mission—Its Scientific Investigations*, K.-P. Wenzel, R. G. Marsden, B. Battrick, Eds. (esa SP-1050, European Space Agency Scientific and Technical Publications Branch, European Space Research and Technology Center (ESTEC), Noordwijk, The Netherlands, 1983), pp. 49–73; S. J. Bame *et al.*, *Astron. Astrophys. Suppl. Ser.* **92**, 237 (1992).
6. A. Balogh *et al.*, *Science* **257**, 1515 (1992).
7. W. C. Feldman *et al.*, *J. Geophys. Res.* **87**, 632 (1982).
8. S. J. Bame *et al.*, *Science* **232**, 356 (1986).
9. G. Paschmann *et al.*, *Nature* **282**, 243 (1979).
10. M. F. Thomsen, *Am. Geophys. Union Monogr. 35* (1985), p. 253.
11. W. C. Feldman *et al.*, *J. Geophys. Res.* **88**, 96 (1983).

12. We thank our colleagues at the Sandia National Laboratories and Los Alamos National Laboratory for engineering support in the design and implementation of the electronic systems of the solar wind plasma experiment for Ulysses. Programming support from K. J. Sofaly (Los Alamos National Laboratory) and R. Sakurai [Jet Propulsion Laboratory (JPL) of the California Institute of Technology] was essential for analysis of the flyby data. The support of the project scientists and the staffs of the Ulysses Project Offices at JPL, ESTEC, and European Space Operations Center is gratefully acknowledged. Work at Los Alamos was carried out under the auspices of the U.S. Department of Energy with financial support from the National Aeronautics and Space Administration (NASA) and work at JPL was carried out under contract to NASA.

28 May 1992; accepted 5 August 1992

Energetic Charged-Particle Phenomena in the Jovian Magnetosphere: First Results from the Ulysses COSPIN Collaboration

J. A. Simpson,* J. D. Anglin, A. Balogh, J. R. Burrows, S. W. H. Cowley, P. Ferrando, B. Heber, R. J. Hynds, H. Kunow, R. G. Marsden, R. B. McKibben, R. Müller-Mellin, D. E. Page, A. Raviart, T. R. Sanderson, K. Staines, K.-P. Wenzel, Margaret D. Wilson, M. Zhang

The Ulysses spacecraft made the first exploration of the region of Jupiter's magnetosphere at high Jovigraphic latitudes (~37° south) on the dusk side and reached higher magnetic latitudes (~49° north) on the day side than any previous mission to Jupiter. The cosmic and solar particle investigations (COSPIN) instrumentation achieved a remarkably well integrated set of observations of energetic charged particles in the energy ranges of ~1 to 170 megaelectron volts for electrons and 0.3 to 20 megaelectron volts for protons and heavier nuclei. The new findings include (i) an apparent polar cap region in the northern hemisphere in which energetic charged particles following Jovian magnetic field lines may have direct access to the interplanetary medium, (ii) high-energy electron bursts (rise times ≤1 minute and energies extending to >~17 megaelectron volts) on the dusk side that are apparently associated with field-aligned currents and radio burst emissions, (iii) persistence of the global 10-hour relativistic electron "clock" phenomenon throughout Jupiter's magnetosphere, (iv) on the basis of charged-particle measurements, apparent dragging of magnetic field lines at large radii in the dusk sector toward the tail, and (v) consistent outflow of megaelectron volt electrons and large-scale departures from corotation for nucleons.

Measurements of the population of high-energy electrons, protons, and heavier nuclei in Jupiter's magnetic field are essential for understanding the energetic and dynamic processes that govern the Jovian magnetosphere. For example, high-energy electrons [energy (E) > ~1 MeV], whose speed is near that of light, are trapped in the Jovian magnetic field and constrained to travel along the field lines. Their flow along the field lines and their intensity levels provide information about both their origins and the large-scale structure of the magnetic field far from the point of observation. Their speed of propagation along the field also makes them sensitive probes of rapid changes in the magnetic field configuration along the field lines on which they are trapped. Considered together with observations from radio, magnetic field, and plasma investigations, measurements of the trapped electrons and nucleons provide the evidence needed to begin to understand the complex flow of energy between particles and electromagnetic fields and radiation that characterizes the Jovian magnetosphere.

Previous missions that penetrated the magnetosphere of Jupiter (Pioneer 10 and 11 in 1973 and 1974, respectively, and the Voyager 1 and 2 missions in 1979) probed the sunward side and the dawn side (Fig. 1) of the magnetosphere. The Ulysses spacecraft investigated for the first time the region at high latitudes on the dusk side and also reached higher latitudes on the day side than any previous flyby. Ulysses has confirmed many results and conclusions from the earlier missions (*1*, *2*) and, through the broader range of sensitivity of its instrumentation and the exploration of new regions of the magnetosphere, has yielded many surprises and new understandings of the energetics and dynamics of the magnetosphere and its high-energy particles. In this paper, we summarize the most significant results concerning the high-energy particles to come from our early analysis of data from the cosmic ray and solar particle investigations (COSPIN) experiment.

J. A. Simpson, R. B. McKibben, M. Zhang, Enrico Fermi Institute, University of Chicago, 933 East 56 Street, Chicago, IL 60637.
J. D. Anglin, J. R. Burrows, M. D. Wilson, Herzberg Institute for Astrophysics, National Research Council of Canada, Ottawa, Canada, K1A 0R6.
A. Balogh, S. W. H. Cowley, R. J. Hynds, K. Staines, Blackett Laboratory, Imperial College of Science and Technology, Prince Consort Road, London, SW7 2BZ, United Kingdom.
P. Ferrando and A. Raviart, Centre d'Etudes Nucléaires de Saclay, Service d'Astrophysique, Bat. 528, 91191 Gif-sur-Yvette, Cedex, France.
B. Heber, H. Kunow, R. Müller-Mellin, Institut fur Reine und Angewandte Kernphysik, Universität Kiel, Olshausenstrasse 40-60, D-2300, Kiel 1, Germany.
R. G. Marsden, T. R. Sanderson, K.-P. Wenzel, Space Science Department of the European Space Agency, European Space Research and Technology Center, Postbus 299, 2200 AG, Noordwijk, Holland.
D. E. Page, European Space Agency at Jet Propulsion Laboratory, 4800 Oak Grove Drive, Pasadena, CA 91109.

*To whom correspondence should be addressed.

Table 1. Cosmic ray and solar particle investigations (COSPIN) sensor systems and participating institutions (*3*). *Z*, atomic number; n, nucleus.

Institution	Instrumentation	Primary particle response in Jovian magnetosphere
Enrico Fermi Institute, University of Chicago	High-energy telescope (HET)	Electrons: $E \gtrsim 1$ MeV
Herzberg Institute of Astrophysics	High-flux telescope (HFT)	Protons: $0.3 < E \lesssim 10$ MeV; also He, CNO, Fe group
Blackett Laboratory, Imperial College	Anisotropy telescopes (ATs)	Protons: $0.7 < E < 6.5$ MeV $Z \geq 2$: 3.1 to 23 MeV
Space Science Department, European Space Agency (ESA), European Space Research and Technology Center (ESTEC)	Low-energy telescope (LET)	Protons: $0.9 < E < 19$ MeV Helium: $1.0 < E < 19$ MeV/n
University of Kiel and Centre d'Etudes Nucléaires de Saclay	Electron telescope (KET)	Electrons: $2 \leq E < 170$ MeV

The COSPIN experiment uses a group of five instruments (Table 1) to measure a wide range of particle species and energies above ~0.3 MeV, with significant overlap between the ranges of sensitivity for the various independent instruments (*3*). As a result of the overlap, new findings can often be simultaneously confirmed by independent measurements. To avoid possible damage from the high-radiation intensities anticipated, we turned off some portions of the COSPIN instrumentation during its passage through the most intense parts of Jupiter's radiation belts. This reduced the range of charged particle energies and the particle types measured during the encounter (Table 1). Evaluation of the instrument performance after the flyby shows that the COSPIN instruments survived the intense radiation levels undamaged.

In an overview (Fig. 2) of energetic proton and electron fluxes measured by two selected COSPIN data channels during the encounter, including the upstream regions beyond the bow shocks, the magnetopause and bow-shock crossings are those identified as clear crossings by the Ulysses plasma investigation (*4*). The proton flux is represented by the F2 counting rate (0.3 to 7 MeV) from the high-flux telescope (HFT), which is immune to electrons and has a linear response over the entire proton flux dynamic range in the magnetosphere, so that no normalization or dead time correction is required for this data channel. The electron flux is represented by the counting rate E4 (2.5 to 7 MeV) from the Kiel electron telescope (KET). During the closest part of the flyby (Fig. 2), the photomultiplier tubes (PMTs) for the KET were turned off, converting the E4 data channel effectively to an integral counting rate above ~2.5 MeV with a somewhat larger geometric factor and with some contribution from protons with energies above 125 MeV. The E4 profiles were corrected to normalize the PMT-off mode to normal mode and to correct for dead time at high electron flux levels. However, uncertainties remain in these corrections.

At the first crossing inbound, the magnetopause was a sharp boundary for electrons (Fig. 2). Outside the magnetopause, the electron flux in interplanetary space and in the magnetosheath was essentially at background levels. If we assume that the magnetopause was stationary, the electron intensity measured by both the high-energy telescope (HET) and KET rose an order of magnitude or more within a few electron gyroradii of the magnetopause, consistent with observations made by the Pioneer and Voyager spacecraft (*1*, *2*). However, there is evidence that the magnetopause was expanding rapidly at the time of the first crossing (*5*) so that the apparent sharpness of the boundary may have been increased by convection of a broader transition region past the spacecraft. A more extended transition region might be consistent with the much smaller intensity changes associated with the magnetopause crossings on days 34 and 35, when, as suggested by tentatively identified additional magnetopause crossings (*4*) not marked in Fig. 2, the spacecraft may have remained in the near vicinity of the magnetopause for an extended period.

In contrast to the electron flux and earlier observations (*1*, *2*), the proton flux did not increase substantially above the ambient flux measured in interplanetary space until ~37 hours after the spacecraft crossed the magnetopause, when on day 35 the proton flux increased by approximately two orders of magnitude in intensity (Fig. 2) above the ambient interplanetary proton flux. This ambient flux was enhanced by more than an order of magnitude relative to quiet times as a result of an interplanetary proton event that was in progress at the time of the magnetopause crossing. Indeed, the intensity of the protons as observed by the HFT, the anistropy telescopes (ATs), and the low-energy telescope (LET) actually decreased on the crossing of the magnetopause inbound, consistent with the partial exclusion of interplanetary low-energy protons from the magnetosphere. The enhanced fluxes may have obscured smaller fluxes of protons of magnetospheric origin near the magnetopause. Even so, there were fewer magnetospheric protons in the

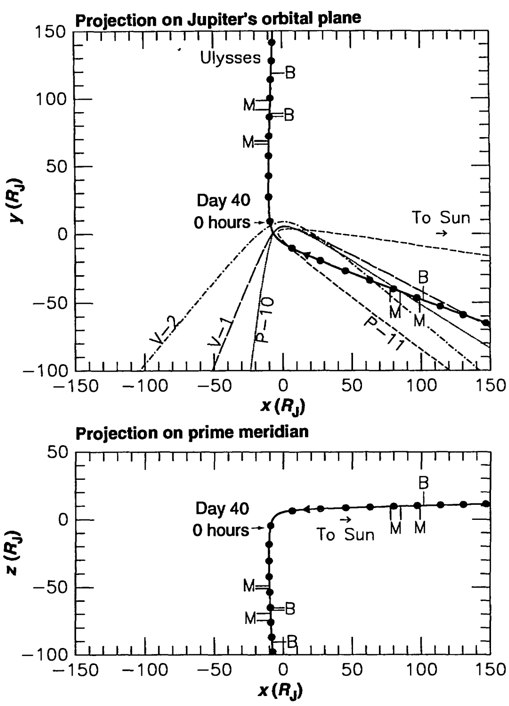

Fig. 1. Equatorial (**top**) and meridional (**bottom**) projections of Jupiter encounter trajectories. The Ulysses trajectory is labeled, and Pioneer 10, Pioneer 11, Voyager 1, and Voyager 2 trajectories are indicated by P-10, P-11, V-1, and V-2, respectively. Bow-shock and magnetopause crossings seen by Ulysses are indicated with B and M. The bow shock and the magnetopause times are taken from table 1 in (*4*) and are based on plasma measurements. The Ulysses trajectory is marked by dots at 1-day intervals, with the point 00:00 UT day 40 identified explicitly.

outer day-side magnetosphere at the time of the Ulysses flyby than during previous flybys (*1, 2*).

On the outbound trajectory, Ulysses made several relatively clear crossings of the magnetopause (*4–6*). In contrast to the inbound observations, significant intensities of electrons and protons were observed up to the magnetopause and also beyond the magnetopause in the magnetosheath on days 44 and 45, before the first bow-shock crossing. The spacecraft crossed the bow shock early on day 45, but after a brief period in the solar wind, the bow shock and magnetopause expanded to overtake the spacecraft for a few hours before its final exit from the magnetosphere late on day 45. During these crossings, few electrons or protons were observed in the sheath, and the magnetopause appeared as a strong boundary for both protons and electrons. The variations in the effect of the magnetopause on Jovian energetic charged particles are not well understood.

At the bow shock, almost no effects were observed on the intensity of energetic particles except for small spikes observed by the HFT in the flux of low-energy protons at the times of the first inbound and last outbound bow-shock crossings on days 33 and 47, respectively (Fig. 2). Other data obtained (*4, 5*) show that the inbound bow-shock normal was quasi-parallel to the magnetic field, whereas the outbound shock normals were quasi-perpendicular to the field. The inbound shock crossing occurred during a period of low solar wind dynamic pressure that was part of a long-lived corotating structure in the solar wind (*4*).

No significant evidence for shock acceleration of energetic particles inbound or outbound was found in data from any of the five COSPIN instruments. On the other hand, there was some evidence on the inbound pass that the low-energy proton flux was enhanced and that protons were streaming away from Jupiter when the extrapolated interplanetary magnetic field direction intersected the bow shock. Some of these enhancements may be the result of particles reflected off or escaping from the bow shock.

In interplanetary space, as for previous Jupiter flybys, enhancements in the electron flux of Jovian origin were observed over several astronomical units upstream, some of which bore the imprint of the planet's rotation in the form of 10-hour variations in the steepness of the electron spectrum. However, the frequency and intensities of the events were much lower than observed during the Pioneer flybys in 1973 and 1974 (*1*).

On its inbound pass through the day-side magnetosphere, Ulysses reached the highest magnetic latitudes yet attained during any flyby of Jupiter. The maximum dipole magnetic latitude of ~49° was reached on day 39 at a radius of ~8.7 Jupiter radii (R_J). At this time (B in Figs. 2 and 3), the fluxes of electrons and protons dropped dramatically. Also at this time, the PMTs of the KET and the HET had been turned off. For the HET, data from interplanetary space in this mode were obtained on day 33 (bars in Fig. 3 indicate the level observed at that time). For the KET, analysis of the response to electrons at the time the PMTs were switched off, together with the calculated increase in geometric factor

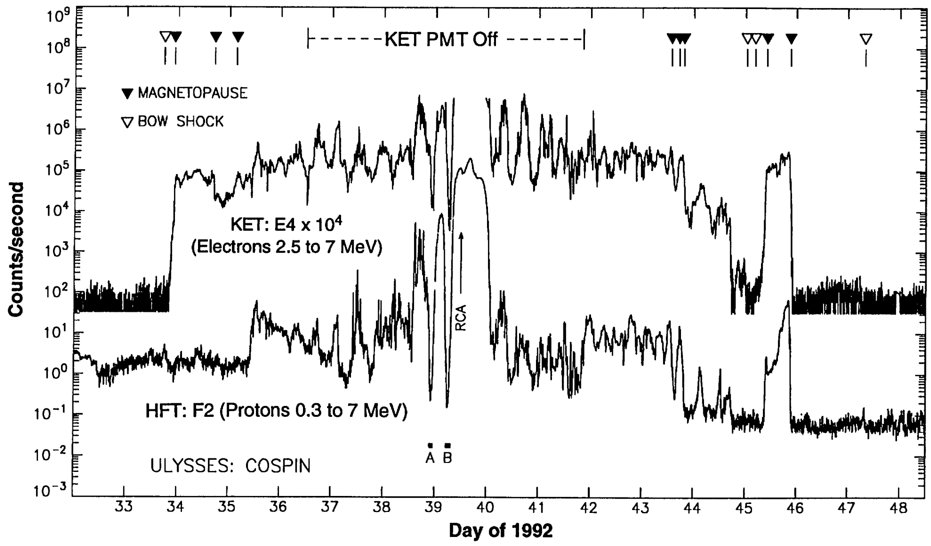

Fig. 2. Overview of the data obtained by COSPIN during the Jupiter encounter represented by two data channels; the omnidirectional counting rates in the KET electron channel (2.5 to 7 MeV) (top) and in the HFT proton channel (0.3 to 7 MeV) (bottom). Periods A and B indicate possible polar cap traversals. The time of closest approach [radius of closest approach (RCA)] is indicated by an arrow. Bow-shock and magnetopause crossings from (*4*) are labeled with open and filled triangles, respectively. For 09:00 to 23:30 UT on day 39, counting rates in all electron channels were saturated, and no useful information was obtained. See Table 1 for identification of the KET and HFT instruments.

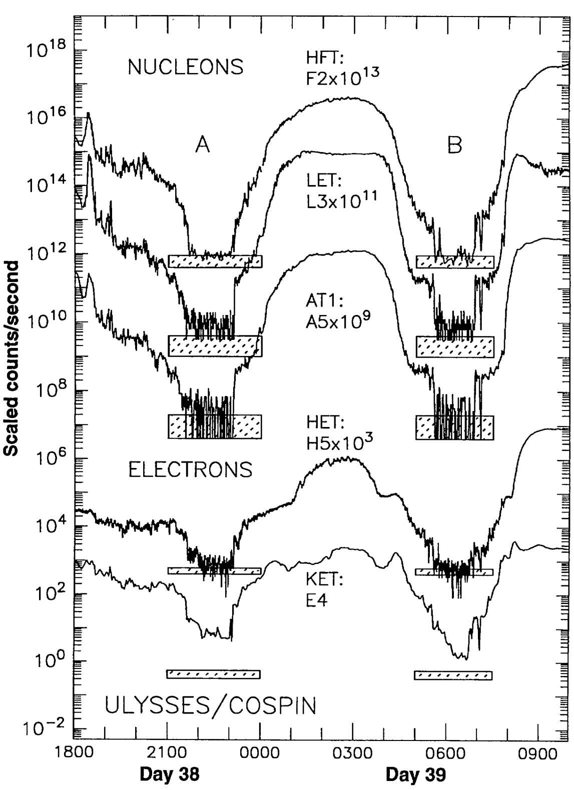

Fig. 3. Scaled counting rates in various particle channels: from top to bottom are HFT protons (0.3 to 7 MeV), LET protons (1.8 to 3.8 MeV), AT protons (3.6 to 6.5 MeV), HET electrons (>8.9 MeV), and KET electrons (2.5 to 7 MeV). The hatched bars near the flux minima for each counting rate indicate the interplanetary flux levels. For the HFT, LET, and AT, these are the fluxes observed on day 46 1992. The interplanetary level of the HET electron channel was taken from day 33 when the instrument was in the same measurement mode as in the period shown. For the KET, the interplanetary levels were computed on the basis of the expected response with the PMTs turned off to the proton and electron intensities measured on day 33. A and B identify the periods similarly labeled in Fig. 2. Hours (UT) are indicated at the bottom.

for response to nuclei above 125 MeV by E4, suggests that the counting rate from interplanetary fluxes of protons and electrons would be in the range shown by the bars below the E4 counting rate trace in Fig. 3.

Although the protons decreased to interplanetary levels, the situation for electrons is less clear. The contribution of electrons and high-energy protons ($E >$ 125 MeV) to the E4 counting rate with the PMTs off suggests this conclusion: the difference by a factor of 2 on day 39 from the counting rate that would be expected as a result of the interplanetary proton and electron fluxes implies that the flux of electrons >2.5 MeV exceeded by a factor of about 20 the interplanetary electron flux measured before entry into the magnetosphere. For the HET, the agreement with the observed interplanetary flux in the same mode clearly does not require any additional electron flux for energies greater than 8.9 MeV.

The rates of increase and decrease on either side of the minimum intensity regions suggest that the spacecraft crossed the high-latitude boundary of stable trapping for energetic particles in Jupiter's magnetosphere and entered a region similar to the polar cap or, possibly, the polar cusp region of Earth's magnetosphere, where particles may have direct access to the interplanetary medium. Additional evidence for this interpretation comes from (i) the decrease of the proton/helium abundance ratio observed by the LET from values near 150:1 in the stable trapping region to values of ~20:1 in the polar cap region, typical of values measured in interplanetary space (*7, 8*), (ii) the disappearance of the corotation anisotropy for low-energy (~1 MeV) protons as measured by the ATs (*9*), and (iii) the appearance of plasma with characteristics typical of the interplanetary medium at ~5 AU (*5*).

During the period of near-interplanetary flux levels, the magnetic field lines threading the spacecraft can be traced to the surface of Jupiter (*10*). Using the O4CS magnetic field model (*11*), we find that the field lines intersect the surface within the auroral oval computed by Connerney *et al.* (*12*) as the high-latitude limit of field lines that close within the magnetosphere (Fig. 4B). Poleward of the auroral oval, energetic charged particles would be expected to have direct access to the interplanetary medium, although the degree of access may depend on particle energy and species, as suggested by the observation by the KET of still significant fluxes of low-energy magnetospheric electrons in this region (as shown by the E4 trace in Fig. 3).

Approximately 8 hours before the maximum latitude was reached, a similar decrease of particle intensities to interplanetary levels was observed (Figs. 2 and 3). At this time [~22:30 universal time (UT) day 38], the spacecraft was at dipole magnetic latitude of ~34° at a radius of ~15 R_J. Also during this period, the model field lines threading the spacecraft lay within the auroral oval computed from the O4CS model (Fig. 4A). In both cases, the period of minimum flux did not extend over the entire time that the spacecraft was on field lines inside the oval. This result suggests that the oval may have been smaller during the Ulysses flyby than is predicted by the model. Concurrent observations of the auroral oval by the Hubble Space Telescope (*13*) may be helpful in resolving this question.

Ten hours earlier, at a radius of ~24 R_J, the spacecraft was also on field lines that extrapolated to the surface within the computed auroral oval. However, the particle intensities remained elevated throughout this period (Fig. 2). These observations suggest that deviation of actual magnetic field lines from those in the model increased with increasing distance from the planet at high latitudes. Possible reasons for such deviation include (i) a variation in the contribution to the magnetic field from the current sheet since the Voyager flyby, on which the O4CS model is based, (ii) the increasing influence of unmodeled currents (for example, in the magnetopause) at larger radii, or (iii) the fact that the Ulysses trajectory lay at higher latitudes than the Voyager trajectory and thus outside the regions of the magnetosphere for which the model was derived.

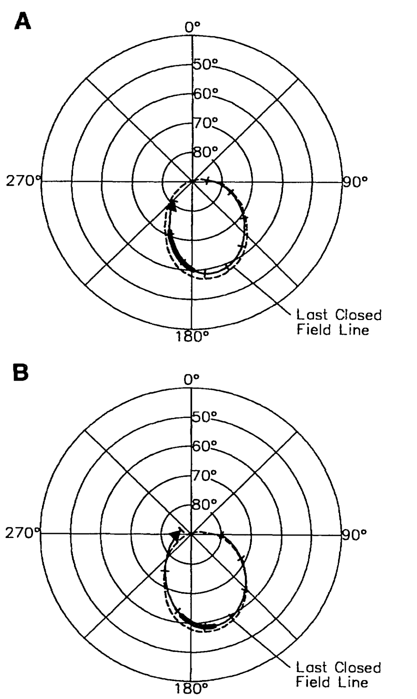

Fig. 4. Footprints on the Jovian surface of magnetic field lines that passed through the spacecraft on day 38 (**A**) (16:00 to 24:00 UT) and day 39 (**B**) (02:00 to 09:00 UT) (solid line), calculated with the use of the O4CS magnetic field model (*11*). Tick marks are placed at 1-hour intervals. The dashed line shows the northern polar auroral oval predicted by the O4CS model (*12*). The thick line on the footprints indicates the regions where near-interplanetary particle flux levels were observed in the magnetosphere. Coordinates shown are Jovigraphic latitude and system III longitude.

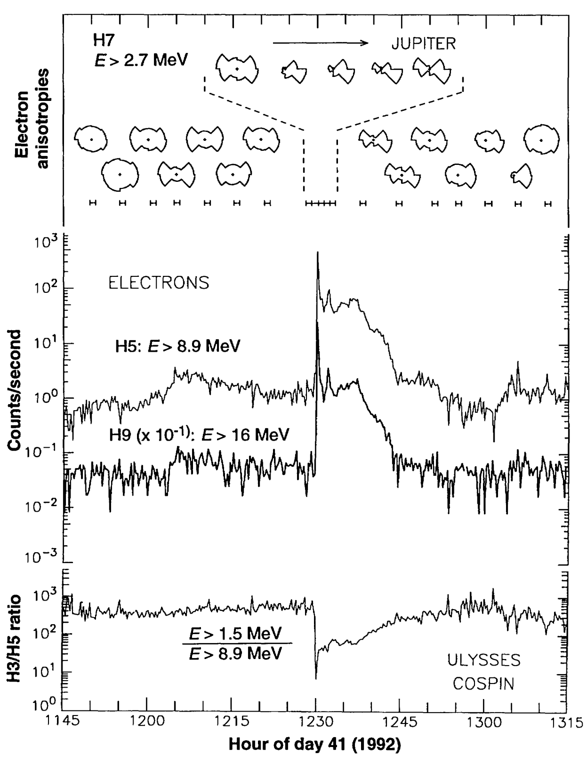

Fig. 5. An example of a relativistic electron burst as seen by the HET. The diagrams on the top show the normalized counting rates in eight sectors of the spacecraft spin during the intervals indicated by the brackets immediately below. The ratio of the counting rate of $E >$ 1.5 MeV electrons to $E >$ 8.9 MeV electrons (bottom curve) shows the hardening of the electron energy spectrum during the burst. The initial flow of electrons in the burst is outward from Jupiter's south pole and develops into bi-directional flow later in the event.

On its outbound pass through the dusk-side magnetosphere at high southern latitudes, Ulysses traversed a region of the magnetosphere not previously explored. The highly variable intensities of the protons and electrons observed after day 40 (Fig. 2) and the multiple crossings of the dusk-side magnetopause and bow shock on the outbound pass make it clear that large-scale dynamical phenomena are occurring on the dusk side as the plasmas, magnetic fields, and energetic particles rotate from the compressed day-side magnetosphere into the extended magnetotail.

A striking discovery made during the outbound pass was the observation of impulsive and sometimes quasi-periodic increases in electron intensity throughout the dusk-side magnetosphere. Particularly clear examples of such bursts occurred on days 41 and 42 (Figs. 5 and 6). Typically, the onset of enhanced intensity was accompanied by strong first- and second-order anisotropies that gradually subsided to the background levels. During the bursts, even when there was primarily strong bi-directional flow along the magnetic field lines, the overall net flow of the electron population was away from the planet along the magnetic field (*14*) (Table 2). Measurements by the KET confirm the measurements from the HET with respect to the high energy and anisotropy of electrons in the bursts. Measurements of nucleons from the ATs, the HFT (Fig. 6), and the LET show that the bursts consist almost entirely of electrons. At least some of these enhancements were correlated with the hot plasma bursts (*15*) and with bursts of radio emission (*16*).

In addition to the large events, there were many small, brief events—for example, between 21:30 and 23:00 UT on day 41 and at about 03:00 and 03:40 UT on day 42 (Fig. 6). These events showed the same rapid rise, hardened electron energy spectrum, and outward-directed anisotropy as the larger events but did not show the extended decay. To estimate the number of bursts, we identified as bursts periods that showed a large statistically significant intensity increase within ~1 min for electrons with energy greater than ~9 MeV accompanied by a significant hardening of the spectrum. A search of the HET data covering both inbound and outbound passes discovered ~100 large and small bursts on the outbound pass but found only one event on the inbound pass through the day-side magnetosphere. No bursts of this kind have so far been identified in the magnetosheath or in interplanetary space. The rapid onset of the events (<~1 min) suggests they may be produced by quasi-periodic explosive magnetic merging in a fashion similar to the impulsive electron acceleration discovered in the magnetotail of Mercury (*17*). However, the anisotropy at onset, directed outward from the planet, seems to require that the acceleration be accomplished at low altitudes on high-latitude magnetic field lines. Rough estimates of the energy and total electron content of typical large bursts such as those shown in Figs. 5 and 6 suggest that these bursts may be a significant source of the relativistic electrons observed in Jupiter's outer magnetosphere and in interplanetary space (*18*).

In addition to the impulsive intensity and spectral variations discussed above, throughout the magnetosphere the intensity and spectrum of high-energy electrons was found to vary with approximately the 10-hour period of Jupiter's rotation. Inside the Jovian magnetosphere, there are two sources of such variations. The first is the inclination (about 10° to the planet's spin axis) of the rotating magnetodisc, or plasma sheet, near the magnetic equator. The magnetodisc will swing toward and away from an observer at a given longitude, with the result that the trapped electron flux and energy spectrum will be a sample of the changing magnetic latitudinal dependence of the trapped electron flux and energy spectrum. The phase of this 10-hour variation changes with changes in the azimuth of the observer's position; the phase also changes sign in passing from, say, the northern to the southern hemisphere of the magnetosphere.

The source of the second variation is changes in the slope of the Jovian electron differential energy spectrum. This variation in the spectrum produces an energy-dependent variation in intensity, which is observed to be strongest at the highest energies and which is separate from the variation controlled by proximity to the magnetodisc. The phase of this 10-hour variation has been found by Pioneer 10 to be independent of spacecraft azimuth inbound on the sunward side and outbound on the dawn side (*19*) and by Pioneer 11 to maintain the same phase in both the northern and southern hemispheres on the sunward side (*20*).

The phase of this spectral variation was found to be locked into the synodic rotation period of Jupiter—that is, phased with respect to the Jovian longitude of the sun-Jupiter line (*20*) and independent of the azimuth of the spacecraft. Pioneer 10 investigations also led to the discovery that relativistic electrons escaped the Jovian magnetosphere to propagate throughout the interplanetary medium with the imprint of the planetary rotation period (*19*). These discoveries were later confirmed by the Voyager 2 spacecraft (*21*). Because the spectral variations seem to depend only on the rotational phase of Jupiter, they appear to reflect a temporal rather than a spatial

Table 2. Characteristics of impulsive electron bursts.

Rise times are of order 1 min or less.
Durations range from ~1 min to ~40 min.
Intensity increases may exceed a factor of 100 above 9 MeV.
Electron energies extend beyond 16 MeV.
Spectrum hardens abruptly at onset.
Strong bi-directional anisotropies are observed, often with strong unidirectional anisotropies directed away from Jupiter at onset.
Bursts may be quasi-periodic, with intervals between bursts of ~40 min.
Bursts are observed almost exclusively on the dusk side during Ulysses flyby.

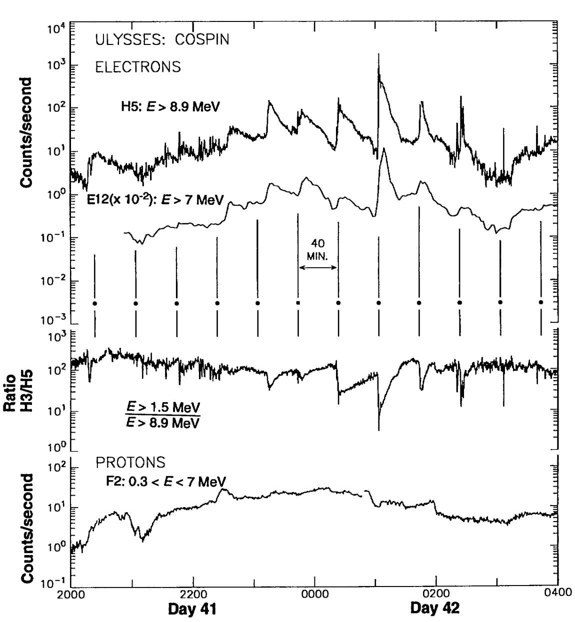

Fig. 6. A quasi-periodic sequence of electron bursts with a period of ~40 min showing electron data channels for the HET and KET and a proton channel from the HFT, demonstrating the absence of protons from the burst. Hours (UT) are indicated at the bottom.

variation and have thus come to be called the "10-hour clock" variations.

By extending observations to the dusk side, the Ulysses flyby provided an opportunity to determine whether this clock is indeed a global magnetospheric phenomenon independent of the magnetodisc. During the Ulysses flyby, the 10-hour variation of spectral slope was derived from the ratio of HET counting rates for low-energy (H3 = $E > 1.5$ MeV) and high-energy (H5 = $E > 9$ MeV) electrons, designated as the ratio H3/H5 (Fig. 7). The maxima in this ratio correspond to maxima in the spectral index, γ, of a power law energy spectrum (that is, $dJ/dE \propto E^{-\gamma}$, where J is flux and γ is the power law constant). A similar analysis was also carried out with the KET on the basis of the ratio of the two electron channels E4 and E12 corresponding to the energies 2.5 to 7 MeV and 7 to 170 MeV, respectively. As for the Pioneer 10 analysis, the successive maxima for these spectral ratios were adopted as markers for the phase of the variation. The first peak in the spectral ratio on the inbound pass (Fig. 7) is the reference time for Ulysses' analysis, and the tick lines shown through the rest of the data in the magnetosphere are based on this starting point. At the times represented by the ticks, the system III longitude (λ_{III}) at the subsolar point was 270°, which is within the general region of the so-called "active" longitudes, as earlier pointed out by Vasyliunas (*22*).

The reference peak for Ulysses occurred less than 30 min from the predicted time for maximum spectral steepness on the basis of counting the 16,058 Jovian synodic (not sidereal) rotation periods (9 hours, 55 min, and 33.12 s) since the reference time defined (*19*) during the inbound of pass of Pioneer 10 in 1973. Because Pioneer 10 (1973) and Ulysses (1992) entered the dayside magnetosphere at nearly the same longitude but in the southern and northern hemispheres, respectively, this agreement between the time predicted from the Pioneer observations and the time observed by Ulysses confirms that the clock phenomenon is independent of the hemisphere of observation.

In Fig. 8, two independent sets of measurements were used to define the times of maximum spectral index, γ_{max}—namely the ratio H3/H5 for the HET and E4/E12 for the KET instruments. When there are clear maxima in the data, the times determined for γ_{max} from the two channels are in agreement. On the outbound pass, because of the rapid magnetic field (*6*) and charged particle flux variations (Fig. 2), the variations in the spectral ratio were noisy, and in some cases maxima could not be identified. Nevertheless, it is clear (Fig. 8) that the 10-hour clock persisted through the outer and middle magnetosphere, including in the magnetosheath on the dusk side. If the variations had been controlled by proximity of the spacecraft to the magnetodisc, there would have been a ~5-hour phase shift after the closest approach and an additional shift of ~3.5 hours from the change in azimuth of the spacecraft's inbound versus outbound trajectories. This was not observed. Thus, the Ulysses observations confirm that the 10-hour clock variations are seen, in phase, on the dusk side of the magnetosphere as well. Although current hypotheses for the origin of the 10-hour clock spectral variations as a global magnetospheric phenomenon account for some aspects of the measurements (*1*, *23*), they still do not appear to explain all the observations derived from the five spacecraft encounters with the Jovian magnetosphere.

In contrast to the spectral variations arising from the clock mechanism, the variations in the flux of high-energy electrons are produced by the superposition of variations controlled by proximity to the magnetodisc and the temporal or clock variations in the spectrum. Thus, the phase of the intensity variations deviates from the phase of the clock variations at different longitudes, reflecting the mix of spatial and temporal effects contributing to the total variation. Where the contribution from the

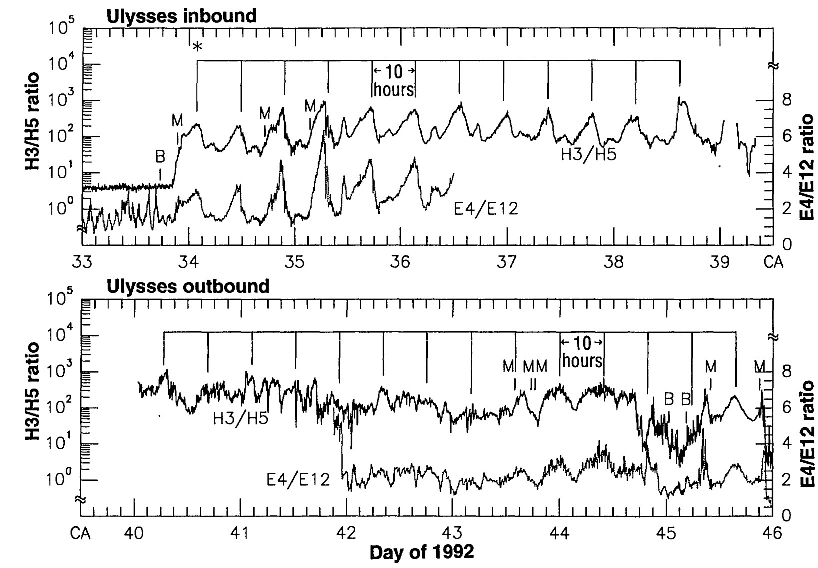

Fig. 7. H3/H5 and E4/E12 ratios of the intensities of low-energy to high-energy electrons, showing the variation of the electron spectrum with Jupiter's synodic rotation period throughout the middle and outer magnetosphere on the morning side and in part of the dusk-side magnetosphere. The asterisk (top) at about UT 01:45 on day 34 1992 was chosen as a reference point for this study. To accommodate the different ranges of variation of the two ratios, we plotted H3/H5 on a logarithmic scale (left), whereas E4/E12 is plotted on a linear scale (right). M and B indicate magnetopause and bow-shock crossings, respectively.

Fig. 8. Times of occurrence of electron spectral index maxima and high-energy electron flux minima relative to the time expected based on the assumption of a strict periodicity of Jupiter's synodic rotation period (9 hours, 55 min, 33.12 s). Magnetopause crossings are indicated by M. Periods outside the magnetopause are shown as hatched bars. The sketch illustrates schematically the distortions of the magnetic field lines from rigid corotation (dashed line) implied by the observations. The dashed circle indicates qualitatively the existence of an inner region in which rigid corotation is observed and outside of which the field lines are dragged toward the tail.

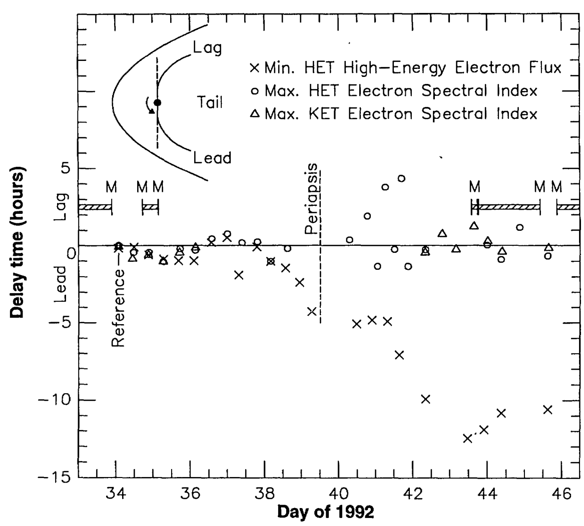

spatial effects is strong, the phase of the high-energy electron intensity variations can be used as a tracer of the distortion of the magnetic field lines that guide the particles.

Inbound, the trajectory azimuth was approximately constant as was the timing of the H5 minima until the spacecraft approached the passage to the southern hemisphere on days 39 and 40. Outbound, the phase change for the intensity minima corresponded to the expected phase change for the spatially controlled variations assuming rigid corotation of the magnetic field until about day 41.5, after which the minima occurred at successively larger intervals of time, Δt, in advance of the time expected for rigid corotation (that is, leading corotation) (Fig. 8). This phase advance with respect to rigid corotation continued to grow outbound to the magnetosheath where Δt reached approximately 10 hours at ~37° south latitude and at ~149 R_J (Fig. 8), so that the intensity and spectral variations were back in the same phase as observed inbound and in interplanetary space.

A similar effect was reported for the dawn-side outbound pass of Pioneer 10 through to the bow shock, except that the time shift of the high-energy electron flux variations relative to corotation was consistent with a lag (the intensity minimum occurring after that expected for rigid corotation) (Fig. 8). This result implied that the magnetic field lines guiding the particles lagged behind the corotation in the outer, dawn-side magnetosphere (*1*, *24*).

The combined results from Pioneer and Ulysses suggest that both the dawn and dusk sides of the outer magnetosphere may be affected by drag from the solar wind beyond about 45 to 50 R_J (Fig. 8), rather than being entirely controlled by planetary rotation (*25*). Independently, the Ulysses magnetic field investigators (*6*, *26*) have reported that on the outbound pass the field deviated from a rigidly corotating model field in a direction consistent with the field lines being dragged toward the tail (*5*). Such a configuration implies the presence of significant field-aligned currents in the dusk-side magnetosphere.

Another tool for investigating the degree to which the outer magnetosphere corotates with the planet is the study of particle anisotropies. Anisotropies measured for nucleons in the day-side outer magnetosphere present a rather complicated picture. Whereas for full corotation near the magnetopause a plasma flow velocity of greater than ~1000 km/s would have been expected, before the large flux increase on day 35 (Fig. 2) the ATs measured only weak anisotropies for ions of 0.7 to 1.3 MeV, corresponding to flows of <~200 km/s that were generally directed opposite to corotation. This result presents a significant contrast to Voyager observations, where near full corotation was observed out to the magnetosphere on the day side (*27*), but is consistent with the Pioneer observations (*28*), where only weak anisotropies were observed at large distances on the day side. After the flux increase on day 35, large flows with significant north-south components, fluctuating on time scales of several minutes, were observed. A strong 10-hour periodicity in the intensity developed during days 36 and 37, and maxima occurred when the spacecraft was near the equatorial plasma sheet. During these intensity maxima, the proton anisotropies were approximately consistent with rigid corotational flow, but at higher latitudes outside the plasma sheet, the flows were weak, similar to those observed in the outer magnetosphere. This pattern is consistent with the expected magnetic connection between the high-latitude middle magnetosphere and the outer magnetosphere. Taken together with the approximately corotational flows observed near the current sheet, these data suggest that the particle bulk flow velocity varies significantly as a function of radius and latitude.

For electrons of several megaelectron volts in energy, the behavior of the anisotropies was more consistent. Almost everywhere in the outer magnetosphere, both inbound and outbound, a small unidirectional or first-order anisotropy directed outward from the planet along the magnetic field was observed by the HET and the KET (*14*). A field-aligned second-order or dumbbell pitch-angle distribution was also usually observed, characteristic of trapped particles mirroring at altitudes below the spacecraft. Similar observations have been reported previously by Sentman *et al.* for the Pioneer 11 flyby (*29*). During the burst events, as discussed above, the forward-backward ratio characterizing the first-order anisotropy often became large, but at almost all other times the outwardly directed intensity was of the order of a few percent larger than the intensity directed toward the planet. These observations suggest that electrons were being injected in a quasi-continuous manner on to high-latitude field lines near the planet, perhaps by low-altitude diffusion from the stably trapped radiation belts as proposed for the recirculation model suggested by Nishida (*30*) or perhaps by acceleration near the feet of the field lines. Absence of a full return flux after mirroring in the opposite hemisphere implies that the electrons were only partially trapped. Such partial trapping suggests that electrons were escaping diffusively near the equatorial plane through the outer magnetosphere and the magnetopause. This suggestion is supported by the observation of primarily first-order anisotropies directed away from Jupiter for electrons in the magnetosheath on the outbound pass (*14*). Calculations of the approximate total outflow of electrons from Jupiter implied by the persistent outward anisotropy suggests that this flow may make significant contributions to the interplanetary Jovian electron flux.

REFERENCES AND NOTES

1. J. A. Simpson and R. B. McKibben, in *Jupiter*, T. Gehrels, Ed. (Univ. of Arizona Press, Tucson, 1976), pp. 738–766.
2. A. W. Schardt and C. K. Goertz, in *Physics of the Jovian Magnetosphere*, A. J. Dessler, Ed. (Cambridge Univ. Press, Cambridge, UK, 1983), pp. 157–196.
3. J. A. Simpson *et al.*, *Astron. Astrophys. Suppl. Ser.* **92**, 365 (1992).
4. S. Bame *et al.*, *Science* **257**, 1539 (1992).
5. A. Balogh *et al.*, *ibid.*, p. 1515.
6. E. J. Smith, K.-P. Wenzel, D. E. Page, *ibid.*, p. 1503.
7. R. G. Marsden *et al.*, paper presented at the meeting of the European Geophysical Society, Edinburgh, Scotland, 6 to 10 April 1992.
8. R. G. Marsden *et al.*, *Eos* **73** (suppl.), 181 (1992).
9. K. Staines *et al.*, *ibid.*, p. 181.
10. R. B. McKibben and J. E. P. Connerney, *J. Geophys. Res.* **91**, 10975 (1986).
11. J. E. P. Connerney, M. H. Acuna, N. F. Ness, *ibid.* **87**, 3623 (1982).
12. ______, *ibid.* **86**, 8370 (1981).
13. J. Caldwell, D. M. Anthony, B. Turgeon, *Eos* **73** (suppl.), 176 (1992).
14. M. Zhang, R. B. McKibben, J. A. Simpson, *ibid.*, p. 182.
15. L. J. Lanzerotti *et al.*, paper presented at the meeting of the European Geophysical Society, Edinburgh, Scotland, 6 to 10 April 1992; *Science* **257**, 1548 (1992).
16. R. J. MacDowall *et al.*, Proceedings of the *Magnetospheres of the Outer Planets Workshop*, University of California at Los Angeles, 22 to 26 June 1992; R. G. Stone *et al.*, *Science* **257**, 1524 (1992).
17. J. Eraker and J. A. Simpson, *J. Geophys. Res.* **91**, 9973 (1986).
18. R. B. McKibben, M. Zhang, J. A. Simpson, H. Kunow, A. Raviart, *Eos* **73** (suppl.), 182 (1992).
19. D. L. Chenette, T. F. Conlon, J. A. Simpson, *J. Geophys. Res.* **79**, 3551 (1974).
20. J. A. Simpson *et al.*, *Science* **188**, 455 (1975).
21. A. W. Schardt, F. B. McDonald, J. H. Trainor, *J. Geophys. Res.* **86**, 8413 (1981).
22. V. M. Vasyliunas, *Geophys. Res. Lett.* **2**, 87 (1975).
23. T. W. Hill, A. J. Dessler, C. K. Goertz, in (*2*), pp. 353–394.
24. R. B. McKibben and J. A. Simpson, *J. Geophys. Res.* **79**, 3545 (1974).
25. J. A. Simpson, paper presented at the meeting of the European Geophysical Society, Edinburgh, Scotland, 6 to 10 April 1992.
26. M. K. Dougherty *et al.*, paper presented at the meeting of the European Geophysical Society, Edinburgh, Scotland, 6 to 10 April 1992.
27. S. M. Krimigis and E. C. Roelof, in (*2*), pp. 106–156.
28. F. B. McDonald, A. W. Schardt, J. H. Trainor, *J. Geophys. Res.* **84**, 2579 (1979).
29. D. D. Sentman, J. A. Van Allen, C. K. Geortz, *Geophys. Res. Lett.* **2**, 465 (1975).
30. A. Nishida, *J. Geophys. Res.* **81**, 1771 (1976).

31. We thank N. Angold, C. Brower, J. Johnson, D. Morris, the Mission Support Area staff, and the ESA and Jet Propulsion Laboratory (JPL) project staff for their efforts during the flyby; the many engineers and technical staff who participated in the design, fabrication, and test of the instrumentation; G. Lentz, M. Perkins, and G. Popelka for their contributions to the operations for the entire

consortium; and J. Connell, S. Ho, H. Boll, and R. Ducros for their help with the data analysis. We also appreciate helpful discussions with J. Connerney on the magnetic field models. The work at the University of Kiel is supported by the Deutsche Agentur für Raumfahrtangelegenheiten GmbH under contract No. 50 ON 9106. The Saclay contribution to this work is supported by the Commissariat à l'Energie Atomique and the Centre National d'Etudes Spatiales. The work at the University of Chicago is supported in part by NASA/JPL contract 955432. The work at Imperial College, London, is supported by a grant from the Science and Engineering Research Council.

1 June 1992; accepted 31 July 1992

Ulysses Dust Measurements Near Jupiter

Eberhard Grün,* Herbert A. Zook, Michael Baguhl, Hugo Fechtig, Martha S. Hanner, Jochen Kissel, Bertil A. Lindblad, Dietmar Linkert, Gudrun Linkert, Ingrid B. Mann, J. Anthony M. McDonnell, Gregor E. Morfill, Carol Polanskey, Reiner Riemann, Gerhard Schwehm, Nadeem Siddique

Submicrometer- to micrometer-sized particles were recorded by the Ulysses dust detector within 40 days of the Jupiter flyby. Nine impacts were recorded within 50 Jupiter radii with most of them recorded after closest approach. Three of these impacts are consistent with particles on prograde orbits around Jupiter and the rest are believed to have resulted from gravitationally focused interplanetary dust. From the ratio of the impact rate before the Jupiter flyby to the impact rate after the Jupiter flyby it is concluded that interplanetary dust particles at the distance of Jupiter move on mostly retrograde orbits. On 10 March 1992, Ulysses passed through an intense dust stream. The dust detector recorded 126 impacts within 26 hours. The stream particles were moving on highly inclined and apparently hyperbolic orbits with perihelion distances of >5 astronomical units. Interplanetary dust is lost rather quickly from the solar system through collisions and other mechanisms and must be almost continuously replenished to maintain observed abundances. Dust flux measurements, therefore, give evidence of the recent rates of production from sources such as comets, asteroids, and moons, as well as the possible presence of interstellar grains.

Ulysses carried a new type of dust detector through the Jovian system. The instrument (hereafter called "DUST") is sensitive to submicrometer- to multimicrometer-sized dust particles. DUST has performed flawlessly at close to its maximum sensitivity since launch. Two results obtained by the sensor include the unexpected detection of meteoroid streams in the outer solar system as well as a relative lack of small dust in the region near Jupiter traversed by Ulysses. Before Ulysses our knowledge about the existence of dust in space near Jupiter was based on two types of observations:

E. Grün, M. Baguhl, H. Fechtig, J. Kissel, D. Linkert, G. Linkert, R. Riemann, N. Siddique, Max-Planck-Institut für Kernphysik, 6900 Heidelberg, Germany.
H. A. Zook, National Aeronautics and Space Administration, Johnson Space Center, Houston, TX 77058.
M. S. Hanner and C. Polanskey, Jet Propulsion Laboratory, California Institute of Technology, Pasadena, CA 91103.
B. A. Lindblad, Lund Observatory, 221 Lund, Sweden.
I. B. Mann, Max-Planck-Institut für Aeronomie, 3411 Katlenburg-Lindau, Germany.
J. A. M. McDonnell, University of Kent, Canterbury, CT2 7NR, United Kingdom.
G. E. Morfill, Max-Planck-Institut für Extraterrestrische Physik, 8046 Garching, Germany.
G. Schwehm, European Space Agency European Space Technology Center, 2200 AG Noordwijk, The Netherlands.

*To whom correspondence should be addressed.

1) Pioneer 10 recorded ten meteoroid penetrations (*1*) and Pioneer 11 recorded five (*2*) during 5-day periods when these two spacecraft flew by Jupiter. Corresponding sensitive areas were: Pioneer 10, 0.13 m^2 and Pioneer 11, 0.5 m^2. The minimum masses that could be sensed at an impact velocity of 20 km/s (comparable to the velocities of impact to be expected during much of the Jovian flyby) were 8×10^{-10} g for Pioneer 10 and 6×10^{-9} g for Pioneer 11.

2) When Voyager 1 flew by Jupiter (*3*), it photographically recorded a relatively bright dust ring between about 1.72 and 1.81 Jovian radii (1 R_J = 71,400 km). Later a tenuous outer extension of that ring was discovered in the photography (*4*) that extended out to about the orbit of Thebe at 3.1 R_J.

The DUST sensor has a 140° conical field of view and is mounted to point nearly perpendicular (85°) to the spacecraft spin axis. The direction of an impact is determined from the spacecraft spin angle at the moment of impact. DUST is a multicoincidence impact-ionization detector (*5*) that senses the ionized plasma generated when a dust particle impacts with high speed upon a hemispherical gold target with a sensitive area of 0.1 m^2. The plasma charges are separated, and three signals can be derived for every impact: a negative charge pulse, a positive ion charge pulse, and a channeltron charge pulse that is derived from part of the positive ions. Through empirical calibration both the particle mass and speed can be derived from the signal amplitudes and rise times (*6*).

There is some noise in the lowest amplitude events. Therefore, we only report on noise-free events that, for those we call "small" events, correspond to an impact mass of about 10^{-14} g at an impact velocity of about 15 km/s. When we better understand which very low amplitude events are truly noise, a lower mass threshold can be established. This will permit publication of higher fluxes. During the Ulysses Jupiter flyby [see (*7*) for trajectory characteristics], the experiment was set to a configuration that balanced instrument safety against sensitivity to dust impacts. To avoid enhanced noise (*8*), the instrument was switched to a reduced sensitivity (threshold mass of about 10^{-13} g to record only "large" impacts) 16 hours before closest approach. At 16 hours after closest approach the instrument was set back to high sensitivity. These precautions resulted in an absence of noise events during the Jupiter flyby. As impact velocities are uncertain to about a factor of 2, impact masses are uncertain by about a factor of 10.

During the first 80 days of 1992 (see Fig. 1A) impact rates from both large and small events display two different modes: one is a slowly varying background mode, and the other is a mode of short-term peaks. We call a sequence of dust impacts a peak if the count rate averaged over three impacts is at least a factor of 10 above the background. There were two peaks of large impacts: one at the beginning of the year consisting of three impacts and one around day 39 consisting of nine impacts. In addition, two peaks of small impacts were recorded: one on day 7 (four impacts) and the other a very pronounced peak during days 70 and 71 consisting of 126 impacts.

The peak centered near day 39 corresponds to the flux near the closest approach to Jupiter, at about the time of equatorial plane crossing. Because of the reduced sensitivity of the instrument, only large impacts could be recorded there. Inside 50 R_J only two impacts occurred on the approach leg while seven occurred on the outgoing leg of the flyby trajectory. The full significance of this is still being investigated.

The spin angles of the dust detector at the times of impact (Fig. 1B) were scattered over nearly the full range of possible values. However, the impacts during peak